Available online at www.sciencedirect.com
SCIENCE DIRECT®
Chemistry and Physics of Lipids 142 (2006) 1–13
CPL
CHEMISTRY AND PHYSICS OF LIPIDS
www.elsevier.com/locate/chemphyslip

Combining precision spin-probe partitioning with time-resolved fluorescence quenching to study micelles Application to micelles of pure lysomyristoylphosphatidylcholine (LMPC) and LMPC mixed with sodium dodecyl sulfate

Miroslav Peric *, Marilene Alves, Barney L. Bales

Department of Physics and Astronomy and The Center for Supramolecular Studies, California State University at Northridge, Northridge, CA 91330-8268, United States

Received 3 October 2005; received in revised form 16 February 2006; accepted 17 February 2006
Available online 28 February 2006

Abstract

Micelles of lysomyristoylphosphatidylcholine (LMPC) and mixed micelles of LMPC with anionic detergent sodium dodecyl sulfate (SDS) have been characterized by spin-probe-partitioning electron paramagnetic resonance (SPPEPR) and time-resolved fluorescence quenching (TRFQ) experiments. SPPEPR is a novel new method to study structure and dynamics in lipid assemblies successfully applied here for the first time to micelles. Several improvements to the computer program used to analyze SPPEPR spectra have been incorporated that increase the precision in the extracted parameters considerably from which micelle properties such as effective water concentration and microviscosity may be estimated. In addition, with this increased precision, it is shown that it is feasible to study the rate of transfer of a small spin probe between micelles and the surrounding aqueous phase by SPPEPR. The rate of transfer of the spin probe di-*tert*-butyl nitroxide (DTBN) and the activation energy of the transfer process in LMPC and LMPC-SDS micelles have been determined with high precision. The rate of transfer increases with temperature and SDS molar fraction in mixed micelles, while it remains constant with LMPC concentration in pure LMPC micelles. The activation energy of DTBN transfer in pure lysophospholipid micelles does not change with LMPC concentration while it decreases with the increasing molar fraction of SDS in mixed LMPC-SDS micelles. Both this decrease in activation energy and the increase in the rate of transfer are rationalized in terms of an increasing micelle surface area per molecule (decreasing compactness) as SDS molecules are added. This decreasing compactness as a function of SDS content is confirmed by TRFQ measurements showing an aggregation number that decreases from 122 molecules for pure LMPC micelles to 80 molecules for pure SDS micelles. The same increase in surface area per molecule is predicted to increase the effective water concentration in the polar shell of the micelles. This increase in hydration with SDS molar fraction is confirmed by measuring the effective water concentration in the polar shell of the micelles from the hyperfine spacing of DTBN. This work demonstrates the potential to design mixed lysophospholipid surfactant micelles with variable physicochemical properties. Well-defined micellar substrates, in terms of their physicochemical properties, may improve the studies of protein structure and enzyme kinetics.

Keywords: Electron paramagnetic resonance (EPR) spectroscopy; Time resolved fluorescence quenching (TRFQ) spectroscopy; Lysomyristoylphosphatidylcholine (LMPC); Mixed LMPC-SDS micelles; Spin probes; Spectral line fitting

* Corresponding author. Tel.: +1 818 677 2944; fax: +1 818 677 3234.
E-mail address: miroslav.peric@csun.edu (M. Peric).

0009-3084/$ – see front matter © 2006 Elsevier Ireland Ltd. All rights reserved.
doi:10.1016/j.chemphyslip.2006.02.003

1. Introduction

Lysophospholipids, amphiphilic molecules consisting of a large polar head group and one long hydrocarbon chain, are found in low concentrations in most biological membranes (Stafford and Dennis, 1988). Unlike the long chain diacyl phospholipids, which in water assemble into bilayer structures, lysophospholipids form micelles above a critical micelle concentration (CMC) (Stafford and Dennis, 1988; le Maire et al., 2000). Due to their surfactant properties (Garavito and Ferguson-Miller, 2001; le Maire et al., 2000) and similarity to phospholipid bilayer structure (Beswick et al., 1999), lysophospholipid micelles have been used in the determination of the structure of small membrane proteins by nuclear magnetic resonance (NMR) spectroscopy (Lauterwein et al., 1979). Lipids, in general, play an important role in the activity of membrane bound enzymes (Gennis, 1989), thus one strategy to study the interactions between lipids and enzymes is to disperse the enzyme in pure lysophospholipid micelles. For instance, the folding mechanism of apocytochrome *c* has been studied in both negatively charged lysomyristoylphosphatidylglycerol (LMPG) (Rankin et al., 1998), and zwitterionic lysomyristoylphosphatidylcholine (LMPC) (Bryson et al., 1999) micelles. Another strategy is to use a mixed micelle assay system (Gennis, 1989) in which a lysophospholipid or phospholipid is mixed with a detergent. Also, numerous experiments have shown that the activity of many phospholipasis in micelles is almost two orders of magnitude faster than in vesicles (Deems, 2000). Due to this fact micellar systems containing phospholipids have become widely used assay systems for kinetic characterization of phospholipasis (Deems, 2000).

Micelle size, which can effect enzyme activity and structure, has been studied by a wide range of techniques (Lauterwein et al., 1979; Bryson et al., 1999; Weltzien et al., 1977; Gow et al., 1990; Hayashi et al., 1994; Bergstrand and Edwards, 2001) for a variety of lysophospholipid micelles. The aggregation numbers of a series of ether-deoxy lysolecithins in aqueous solution at 37 °C were extrapolated from Zimm plots of light scattering data (Weltzien et al., 1977). The size of dodecylphosphocholine (DPC) micelles in a 0.02 M DPC solution in 0.05 M phosphate buffer, pH 7, at 20 °C was measured by both ultracentrifugation and quasi-elastic light scattering (Lauterwein et al., 1979). The aggregation numbers of lysolauroylphosphatidylcholine (LLPC) and LMPC micelles were measured by sedimentation equilibrium (Gow et al., 1987; Gow et al., 1990). Light scattering was used to measure the size of 1-palmitoyl-*sn*-glycerol-3-phosphocholine (LPPC) micelles in water as a function of temperature (Hayashi et al., 1994). Since the literature on aggregation numbers of lysophospholipid micelle is not extensive, and reported aggregation numbers are sometimes very variable (le Maire et al., 2000) there is still a need for careful measurement of lysophospholipid aggregation numbers, as well as other physicochemical properties of these micelles.

A variety of techniques can be used to study the physicochemical properties of phospholipid aggregates (Cevc, 1993). One of these, often used to study aggregates, including vesicles and micelles, is the spin probe electron paramagnetic resonance (EPR) technique (Berliner, 1976; Goñi and Alonso, 2000), because spin probes are sensitive and informative "reporters" of their environment. The spin-probe partitioning electron paramagnetic resonance (SPPEPR) method has been successfully applied to study the phase transitions of biological (Hubbell and McConnell, 1968) and model membranes (Shimshick and McConnell, 1973). This method is based on the use of small nitroxide spin probes, which partition into both hydrophilic and hydrophobic environments (Griffith et al., 1974; Schreier et al., 1978). Since the probe is distributed in those two distinctly different environments, the observed spectrum is a superposition of two isotropic triplets originating from the probe in the two environments. The same approach has been attempted in classical micellar solutions (Atherton and Startch, 1971; Oakes, 1972), but with limited success.

Also, the SPPEPR method has been applied to study the solubilization of lipids and the accessibility of an enzyme to the lipid in a model bile solution composed of lecithin and bile salt (Uematsu et al., 1995). Unfortunately, the EPR spectrum of the spin probe used, 2,2,6,6-tetramethyl-1-piperidinyloxy (TEMPO), had only the two high field EPR lines partially resolved, while the other two doublets were completely coalesced, which made the analysis of the EPR data difficult and imprecise. The lifetime of TEMPO in the micellar phase was estimated (Uematsu et al., 1995) by means of line shape analysis of McConnell (1958). The estimated lifetime was very likely in error since the EPR lines were assumed to be homogenously broadened, because it is well established that the EPR lines of TEMPO are inhomogeneously broadened (Bales, 1989). Also, the rotational dynamics of the spin probe in both environments were not measured independently. Because the rotational dynamics had to be simulated, introducing adjustable parameters in addition to the lifetime of the probe in each environment, uncertainties could enter into the values of the extracted lifetimes.

In recent years, it has been shown that the physicochemical properties of the water interface of a variety of aggregates from micelles to vesicles can be studied with high precision by employing spectral line fitting in the spin probe EPR technique provided motionally narrowed EPR spectra are observed (Bales et al., 1998a; Bales et al., 2000; Peric et al., 2005). For example, using a nitroxide spin probe attached to a long hydrocarbon chain, which preferentially dissolves in the hydrophobic surfactant aggregate, it has been found that the hydration and fluidity of the surface of sodium dodecyl sulfate (SDS) micelles were related to the micelle size (Bales et al., 1998a) and micelle shape (Ranganathan et al., 2001). In self-aggregating assemblies, a spin probe with a long hydrophobic chain often does not give a fast motional EPR spectrum that can be analyzed with high precision. This was one motive for the development of SPPEPR (Peric et al., 2005) for more ordered dynamic aggregates (Gil et al., 1998) such as vesicles. SPPEPR, employing the spin probe di-*tert*-butyl nitroxide (DTBN), has been successfully applied to the study of the hydration properties of the surface of two model membrane vesicles (Peric et al., 2005).

The purpose of the present work is three-fold: (1) to demonstrate that SPPEPR may be successfully applied to micelles, yielding EPR parameters of high precision provided that the analysis is carried out in such a way as to minimize the number of adjustable parameters, (2) to characterize in detail the physicochemical properties of pure LMPC and mixed LMPC-SDS micelles by utilizing the SPPEPR and the time-resolved fluorescence quenching (TRFQ) techniques, and (3) to combine the results from (2) to provide a consistent model of the transfer of the spin probe between the micelle and aqueous phases. Items (2) and (3) provide the basis for varying the physicochemical properties of micelles to be used in the study of enzymatic reactions.

2. Materials and methods

2.1. Materials

Lysomyristoylphosphatidylcholine (LMPC, 1-myristoyl-2-hydroxy-*sn*-glycero-3-phosphocholine) was purchased from Avanti Polar Lipids Inc. (Alabaster, AL). Molecular biology reagent SDS, 99%, was purchased from Sigma Chemical Comp. (St. Louis, MO) and the spin probe DTBN was obtained from Molecular Probes (Eugene, OR). The fluorescence probe pyrene (optical grade) and the quencher 1-dodecylpyridinium chloride were from Aldrich (St. Louis, MO). The buffer system used was Hepes (4-(2-hydroxyethyl)-1-piperizineethanesulfonic acid) adjusted with NaOH to pH 7.4. Polytetrafluoroethylene (PTFE) tubing was purchased from Zeus Inc. (Orangeburg, SC).

2.2. Micelle preparation

A stock solution of DTBN in ethanol was added to vials and then dried under a stream of dry, pure nitrogen gas. Then, LMPC and 20 mM Hepes buffer were added. After stirring this solution gently for about 1 h, SDS was added to yield a total lysophospholipid-SDS concentration of 100 mM and a DTBN concentration of 0.25 mM. A few experiments using a DTBN concentration of 0.13 mM were run to check for possible effects of spin–spin interactions. This solution was stirred overnight. SDS molar fractions of 0, 0.25, 0.50 and 1 were studied.

The samples were drawn into 15-cm PTFE tubes of 0.5 mm i.d. and 0.08/0.13 mm wall thickness, whose ends were folded and tightened with a strip of parafilm (American National Can, Greenwich, CT) and melted with a Bunsen burner.

2.3. Methods: (a) EPR measurements

EPR spectra were measured at X-band using a Bruker ESP 300 spectrometer interfaced with a Bruker computer and equipped with a Bruker variable temperature unit (model B-VT-2000). The PTFE tube with the micelle/DTBN solution was placed inside a quartz tube (Wilmad Glass Co Cat No. 412) with a hole in the bottom, which was then inserted in the variable-temperature Dewar inside the EPR cavity. Since the temperature unit uses a stream of nitrogen gas to regulate the temperature inside the EPR cavity, the sample arrangement with gas permeable PTFE tubing allows for deoxygenating the sample (Peric et al., 2005; Plachy and Windrem, 1977). Deoxygenation increases the resolution of the EPR spectrum by removing the line broadening due to paramagnetic oxygen (Hyde and Subczinski, 1989). The temperature of the sample was monitored by an Omega temperature indicator (model DP41-TC-S2) and was kept constant within $\pm 0.2\,^{\circ}C$. After changing the temperature, the sample was equilibrated for at least 5 min. Second harmonic EPR spectra were acquired for each sample using a sweep time of 84 s; microwave power, 5.03 mW; time constant, 20.5 ms; sweep width, 50.2 G; modulation amplitude, 0.506 G; five spectra were collected for each sample. The sweep width of each spectrum was measured with a Bruker NMR Gaussmeter in the 1-mG resolution mode and was averaged over several experiments.

Second harmonic SPPEPR spectra, which are superpositions of the signal in the micelle and in the aqueous phase, were analyzed as described previously (Peric et al., 2005). To simplify the language in this paper, we refer to these signals as the "micelle" and the "water" signals, respectively. Thus, for example, "the high-field water line" means the high-field EPR line of the spectrum due to DTBN in the aqueous phase of the micellar solution. In addition, the computer program that was used in the previous work (Peric et al., 2005) has been improved in several ways. Firstly, the fitting function, written in terms of unit-integrated intensity (Halpern et al., 1993), fits the whole EPR spectrum at once. Secondly, since we use the concentration of DTBN below a concentration which produces spin exchange line broadening (Bales and Peric, 1997) we assume that the unit-integrated intensity is the same for each EPR line belonging to the spectrum originating from each environment. Thirdly, carbon-13 EPR lines due to the natural abundance of ^{13}C in the nitroxide probe were added to the fitting function (Smirnova et al., 1995) for both the micelle and water spectra. As the number of fitting parameter increases, fitting becomes more susceptible to initial guesses for the parameters, especially if the lines overlap. Since the C-13 lines in the case of the high-field lines overlap with nitrogen EPR lines, and are almost two orders of magnitude smaller than the nitrogen EPR lines, their output parameters are more affected than the parameters of the nitrogen EPR lines. We found out by trial and error that it is better to minimize the number of fitting parameters, thus the intensity and hyperfine coupling constant were kept the same for both the micelle and water ^{13}C EPR lines, respectively.

It is critical to use an accurate line shape in the fitting function in order to be able to separate the inhomogeneous broadening (Gaussian) from the homogenous broadening (Lorentzian) (Bales, 1989). Relaxation times are derived from the Lorentzian components, thus the accuracy of these times is limited by our ability to separate the two components. Therefore, fourthly, to improve the precision of the extraction of the Lorentzian linewidth from the observed peak-to-peak linewidth (Bales, 1989), we deduce the value of the Gaussian linewidth by exploiting the fact that it is proportional to the nitrogen hyperfine coupling constant as is shown in Fig. 1.

Fig. 1 shows the Gaussian peak-to-peak linewidth corrected to zero amplitude of modulation $\Delta B_{pp}^{G}(B_m = 0)$ as a function of A_0 of DTBN in dioxane–water mixtures. The hyperfine coupling constant A_0, defined as one-half separation of the high- and low-field lines, and Gaussian peak-to-peak linewidth ΔB_{pp}^{G} of DTBN in a series of dioxane–water mixtures were measured

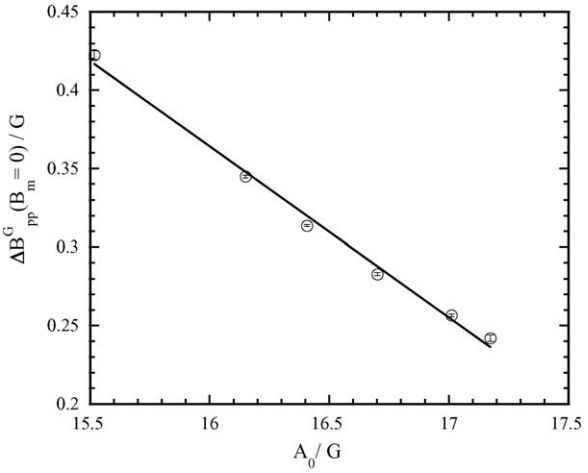

Fig. 1. The Gaussian peak-to-peak linewidth corrected to zero amplitude of modulation $\Delta B_{pp}^{G}(B_m = 0)$ as a function of the hyperfine coupling constant A_0 of DTBN in dioxane–water mixtures. Error bars are standard deviations of five measurements. The solid line is a linear least-squares fit to the data. $\Delta B_{pp}^{G}(B_m = 0) = 2.108 - 0.109A_0$ (coefficient of correlation $r = 0.997$).

as described in detail previously (Halpern et al., 1993). The second harmonic EPR spectra of DTBN were fitted to a sum of Lorentzian and Gaussian functions, which is an excellent approximation to the Voigt line shape that is, in turn, an excellent description of the EPR line shape of most nitroxides in the fast motional regime (Bales, 1989) (Halpern et al., 1993). The solid line is a linear least squares fit to the experimental data given by $\Delta B_{pp}^{G}(B_m = 0) = 2.108 - 0.109A_0$ (coefficient of correlation, $r = 0.997$). These intercept and slope values are in good agreement with those (Bales, 1989) estimated from the data measured for DTBN by Windle (1981), 2.270 and 0.1169 G. We note that the same linearity was observed for the nitroxide spin probe 4-protio-3-carbamoyl-2,2,5,5-tetraperdeuteromethyl-3-pyrroline-1-yloxy (Bales et al., 1992) thus this empirical linearity may hold in general for nitroxides as suggested previously (Bales, 1989).

The values of the Gaussian linewidth in Fig. 1 were corrected for the Gaussian modulation broadening. Since in this work we use the second harmonic representation, we had to investigate whether the effect of field modulation on Gaussian modulation broadening in the second harmonic is the same as in the first harmonic (Bales et al., 1998b). We have confirmed this to be the case; that is,

$$\Delta B_{pp}^{G}(B_m)^2 = \Delta B_{pp}^{G}(0)^2 + \kappa^2 B_m^2 \quad (1)$$

where $\Delta B_{pp}^{G}(B_m)$ is the Gaussian linewidth observed with modulation amplitude $B_m/2$, $\Delta B_{pp}^{G}(0)$ is the

Gaussian linewidth in the limit of zero modulation, and the constant κ is 1/2.54.

A spin probe that exists in two different environments such as micelle and water and undergoes reversible transfer between them may give rise to an EPR spectrum that is a sum of two isotropic triplets originating from the probe in the two environments. The spin probe (SP) transfer process in a micellar solution can be represented as

$$\text{SP in micelle} \underset{k_W}{\overset{k_M}{\rightleftarrows}} \text{SP in water}$$

where k_W is the rate of transfer from water to micelle, and k_M the rate of transfer from micelle to water. As long as the transfer rate between the two environments is slow compared to $\gamma\Delta B$, where $\gamma = 1.76 \times 10^7\ \text{s}^{-1}\ \text{G}^{-1}$ is the magnetogyric ratio and ΔB is the field separation between the lines, one observes two distinct EPR lines. Assuming that the steady state is reached and the thermal equilibrium between spin probes is maintained, according to the method of McConnell (1958) based on the modified Bloch equation, the EPR spectrum is given by (Weil et al., 1993):

$$G = G_M + G_W = iB_1 M_z^0 \frac{\begin{array}{c} P_M\gamma_M(\alpha_W + k_M + k_W) \\ +P_W\gamma_W(\alpha_M + k_M + k_W) \end{array}}{(\alpha_M + k_M)(\alpha_W + k_W) - k_M k_W} \quad (2)$$

$$P_M + P_W = 1 \quad (3)$$

$$P_M k_M = P_W k_W \quad (4)$$

where G is the total complex transverse magnetization, G_M and G_W are the magnetizations in the micelle and water, respectively; B_1 is the microwave magnetic field; M_z^0 is the z-component of the equilibrium magnetization; P_M and P_W are the probabilities of DTBN being in the micelle and water, respectively; $\alpha_M = (1/\tau_{2M}) - i\gamma_M(B_M - B)$ and $\alpha_W = (1/\tau_{2W}) - i\gamma_W(B_W - B)$ where relaxation times τ_{2M} and τ_{2W} represent the inverse Lorentzian linewidths of the DTBN in the micelle and water, and the micelle and water EPR lines are at resonance fields B_M and B_W; B is the external magnetic field; $\tau_M = 1/k_M$ and $\tau_W = 1/k_W$ are the average lifetimes of DTBN in the micelle and water, respectively.

2.4. Methods: (b) TRFQ measurements

A stock solution of pyrene in spectroscopic grade ethanol was prepared and kept in the freezer until needed. The appropriate amount of stock solution was weighed into a vial, and the solvent was removed by a stream of nitrogen. To ensure that the fraction of micelles with two or more pyrene molecules is negligible, the concentration of pyrene in the TRFQ samples was kept at about one hundredth of the concentration of micelles. Then, the required amount of LMPC and buffer were added to this vial and stirred gently overnight. The quencher 1-dodecylpiridinium chloride was weighed in a vial, and a portion of pyrene/LMPC solution was added to approximately one quencher per micelle and followed by stirring for 2 h. Finally, the TRFQ samples were degassed in the freeze–pump–thaw system and equilibrated with argon.

TRFQ measurements were obtained using a computer controlled time-correlated single-photon counting spectrophotometer FL900 from Edinburgh Analytical Instruments (Edinburgh, UK) equipped with a hydrogen filled flash lamp nF900 at a pressure of 0.38 bar. The pulse repetition rate of the lamp was 40 kHz. The fluorescence excitation wavelength was 334 nm, while the emission wavelength was 394 nm. The slit width and the excitation level were adjusted so that the photon count rate did not exceed 800 cps to avoid pulse pile up problems. A PolyScience Digital Temperature Controller Model 9510 (Niles, IL) was used for all TRFQ measurements.

The time-dependent fluorescence decay curves of pyrene in LMPC micelles were obtained in the presence and absence of quencher. The curves were then least-squares fitted to the Infelta–Tachiya equation (Infelta et al., 1974; Tachiya, 1975):

$$I(t) = A_1 \exp\{-A_2 t + A_3[\exp(-A_4 t) - 1]\} \quad (5)$$

with

$$A_2 = k_0 + \frac{k_q k_- < N_q >}{(k_q + k_-)}; \qquad A_3 = \frac{k_q^2 < N_q >}{(k_q + k_-)^2};$$

$$A_4 = k_q + k_-$$

where $A_1 = I(0)$ is the initial fluorescence intensity, $< N_q >$ is the average number of quenchers per micelles and is given as the ratio of the quencher concentration to the concentration of micelles, k_0 is the unquenched decay rate of the probe, k_q is the first order rate constant for quenching in a micelle with one quencher and k_- is the exit rate constant of a quencher from a micelle. Assuming the quencher does not migrate from one micelle to another appreciably, k_- becomes negligible. In this case, the expressions for the A-coefficients reduce to $A_2 = k_0$, $A_3 = < N_q >$ and $A_4 = k_q$. The fits yielded the values of A_2, A_3, and A_4 from which the aggregation numbers were calculated according to $N = A_3$[lysoPC]/[Q], where

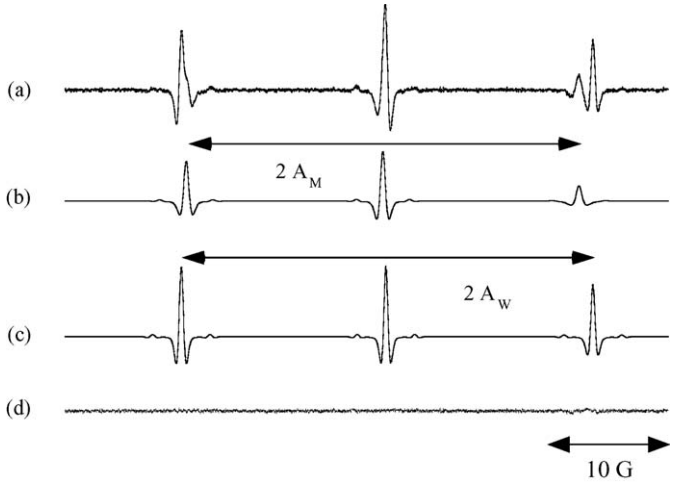

Fig. 2. (a) Experimental second harmonic SPPEPR spectrum of DTBN in 100 mM LMPC micelles at 25 °C equilibrated with nitrogen. The SPPEPR spectrum of DTBN originating from the micellar phase (b), and the aqueous phase (c). (d) The difference between the experimental spectrum and the sum of the spectra (b) and (c). A_M and A_W are one half the distance between the outer lines of the EPR signal originating from the micellar and aqueous phases, respectively.

[LMPC] and [Q] are the molar concentrations of the LMPC and quencher, respectively.

3. Results and discussion

A typical second harmonic SPPEPR spectrum of DTBN in 100 mM LMPC micelles at 25 °C equilibrated with nitrogen is displayed in Fig. 2a. The spectrum was least-squares-fitted to a sum of Gaussian and Lorentzian lineshapes as described previously in Section 2. The best fit to this experimental spectrum is shown in Fig. 2b and c, showing the micelle (Fig. 2b) and water (Fig. 2c) spectra, respectively. The hyperfine coupling constants A_M and A_W are defined as shown; one-half the difference in the resonance fields of the outer lines of the EPR signal in the two respective phases. The excellence of the fit is illustrated in Fig. 2d, which shows the difference between the experimental spectrum and the sum of the water and micelle spectra.

SPPEPR experiments were performed as a function of temperature in steps of 5 °C from 5 to 50 °C. Fig. 3 shows selected EPR spectra of DTBN in a 100 mM solution of LMPC obtained at different temperatures. The most pronounced changes as a function of temperature can be observed visually on the high field EPR lines which are well separated, Fig. 3. Clearly simple methods of analyzing the spectra in Fig. 3 would be of limited use; precise details are only available from fits. As long as the two lines of a doublet are well separated, Eq. (2) gives simple closed expressions for the transfer line broadening and the separation of the two lines (Weil et al., 1993). When the two lines overlap, as in the case of the low- and center-field lines, our analysis indicates that the doublets can still be fitted to a superposition of two lines, but there are no simple relationships for the transfer line broadening and the line separation. Thus, it is obvious from Fig. 3 that only the high-field doublet is in the slow transfer limit implying that it is the most suitable for analysis.

Fig. 4a shows peak-to-peak Lorentzian linewidth ΔB_{pp}^{L} of the high-field water EPR signal in pure LMPC micelles at various surfactant concentrations as a function of temperature. For comparison, the variation of

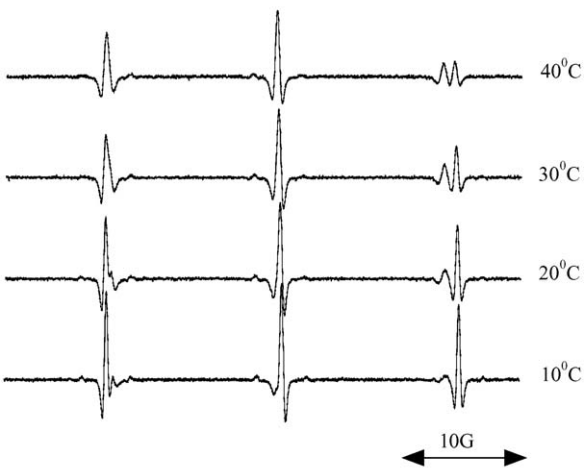

Fig. 3. Selected SPPEPR spectra of DTBN in a 100 mM solution of LMPC obtained at different temperatures.

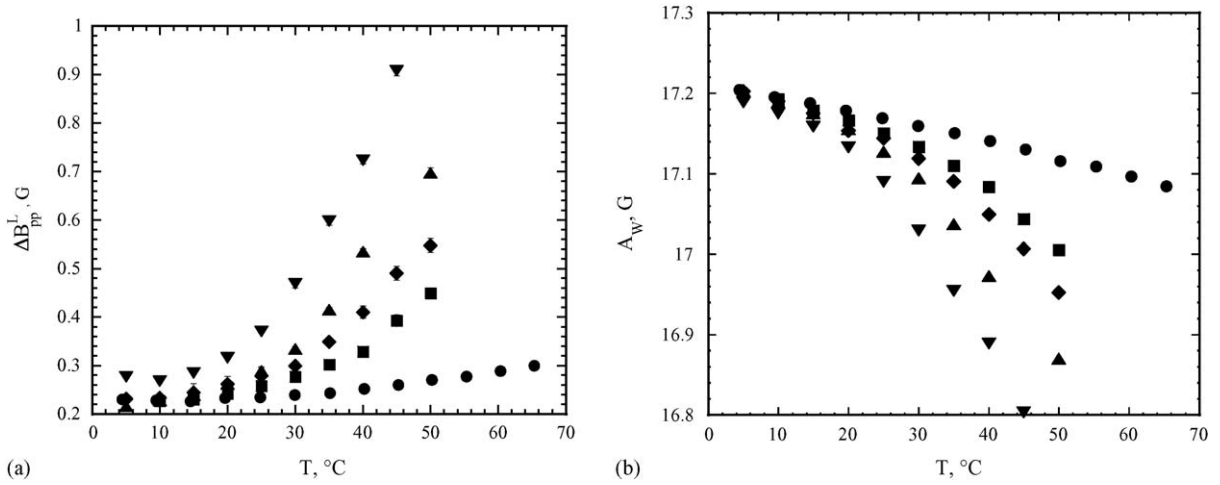

Fig. 4. (a) Peak-to-peak Lorentzian linewidth ΔB^L_{pp} of the high-field water signal in pure LMPC micelles and in Hepes buffer as a function of temperature at various LMPC concentrations. Note the extraordinary precision obtainable from SPPEPR: The entire extent of the ordinate is a mere 0.8 G. (b) The nitrogen hyperfine coupling constant A_W of the water signal in pure LMPC micelles and Hepes buffer as a function of temperature at various LMPC concentrations. (●) Hepes, (■) 50 mM, (♦) 75 mM, (▲) 100 mM, and (▼) 150 mM. Error bars are standard deviations of five measurements, and are often smaller than the size of the symbols.

ΔB^L_{pp} with temperature in Hepes buffer is shown as solid circles. The increase in ΔB^L_{pp} of the water high-field EPR line in the SPPEPR spectrum of LMPC micelles is significantly greater than that in pure Hepes solution. We measured the EPR spectral parameters of DTBN in both water and Hepes buffer, and found that they are the same within experimental error. Thus the terms water and Hepes solution are used interchangeably in the paper. As can be seen from Fig. 4a, ΔB^L_{pp} of the high-field water line increases with the concentration of LMPC.

Fig. 4b shows the hyperfine spacing A_W of DTBN at different LMPC concentrations and water as a function of temperature. The resonant position of the water high field EPR line is shifted inward compared to that of DTBN in pure Hepes solution measured at the same temperature. This decrease in A_W is contrary to that observed in the case of phospholipid vesicles where it was found that the value of hyperfine coupling constant in the aqueous phase of the vesicle sample is the same as in pure Hepes solution (Peric et al., 2005).

Both line broadening and line shifts can be caused by electron spin exchange (Bales and Peric, 1997). We have eliminated this possible explanation of the results in Fig. 4 in two ways. First, the DTBN concentration was reduced by one-half, yielding identical spectra. Second, spin exchange can be detected in a single spectrum by the presence of a characteristic spin exchange-induced "dispersion" (Bales and Peric, 1997). The absence of this dispersion component, which would be easily detected under these conditions, confirms that the effects in Fig. 4 are not due to spin exchange.

We propose that these effects are due to a rapid transfer of the DTBN molecules between the micelle and aqueous phases on an EPR time scale causing the line shift and broadening (Weil et al., 1993; Gutowsky and Holm, 1956; Rogers and Woodbrey, 1962). Assuming that the value of the nuclear spin does not change during the environment transfer, the peak-to-peak transfer broadening δB_W of the water EPR line can be found from:

$$\delta B_W = \Delta B^L_{pp}(\text{water} - \text{micelle}) - \Delta B^L_{pp}(\text{water}) \quad (6)$$

where $\Delta B^L_{pp}(\text{water} - \text{micelle})$ is the peak-to-peak Lorentzian EPR linewidth from the aqueous phase in the micelle sample and $\Delta B^L_{pp}(\text{water})$ is the peak-to-peak Lorentzian linewidth in pure water. The Lorentzian linewidth, $\Delta B^L_{pp}(\text{water})$, separates the contribution of the effect of the molecular tumbling motion of DTBN to the high field EPR linewidth (Nordio, 1976) from the broadening due to the transfer. Eq. (6) is valid only in the slow transfer limit. The rate of DTBN transfer from water to micelle k_W is then given by (Weil et al., 1993):

$$k_W = \frac{\sqrt{3}}{2}\gamma\delta B_W \quad (7)$$

The aforementioned analysis cannot be applied to the broadening of the high field micelle EPR line, because we do not have a solution representing the micellar

environment in which we can measure the effect of the molecular tumbling motion. If the probabilities P_M and P_W are known, the rate of DTBN transfer from micelle to water k_M can be found from Eq. (4), as $k_W(P_W/P_M)$. The probabilities can be found from the unit-integrated intensities of the EPR spectra in the micelle and water. Thus the probability of DTBN being in the micelle is given by $P_M = I_M/(I_M + I_W)$, where I_M and I_W are the integrated intensities of the micelle and water EPR spectra, respectively. This probability is usually reported as a partition ratio (Peric and Bales, 2004; Riske et al., 1999), while the probability of DTBN being in the water is $P_W = 1 - P_M$. Fig. 5 shows P_M as a function of LMPC concentration. As expected, the partitioning of DTBN into the micellar phase increases linearly with increasing LMPC concentration. Within experimental error, the value of P_M is constant with temperature. Thus, the values in Fig. 5 are the averages over all temperatures. The error bars, which represent the standard deviations, indicate that the error in estimating the value of P_M is about ±5%. The values of P_M for mixed LMPC-SDS micelles did not change with SDS concentration, they were found to be within experimental error of the value for 100 mM pure LMPC micelles, which was expected as they all had the same total surfactant concentration.

Fig. 6a shows the rate of transfer of DTBN from water to the micelle in pure LMPC, at different LMPC concentrations as function of the reciprocal of temperature. The solid lines are the fits to the Arrhenius equation:

$$k_W = A\, e^{-E_A/RT} \quad (8)$$

The correlation coefficients for the fits are all greater than or equal to 0.99. The activation energy E_A represents the height of the barrier restricting the transfer of DTBN from water to the micelle. Since the estimated error in δB_W is usually about 10 mG, the values of the broadening which are less than 20 mG were not used in the calculations of the activation energy.

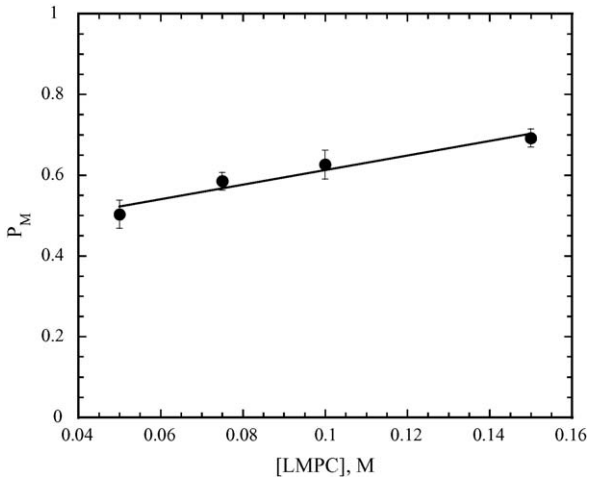

Fig. 5. The probability of DTBN being in the micelle (partitioning ratio) as a function of the concentration of LMPC. Values and error bars are the averages of the values at all the temperatures and their standard deviations. The solid line is a linear least-squares fit to the data $P_M = 0.43 + 1.80$ [LMPC] (coefficient of correlation $r = 0.97$).

According to Eq. (2) (Weil et al., 1993; Gutowsky and Holm, 1956), the separation of the two lines corresponding to the two forms decreases with increasing rate. Thus, the change in separation can, in principle, be used to measure the rate of transfer (Gutowsky and Holm, 1956; Rogers and Woodbrey, 1962). We have observed that the separation between the water and micelle high

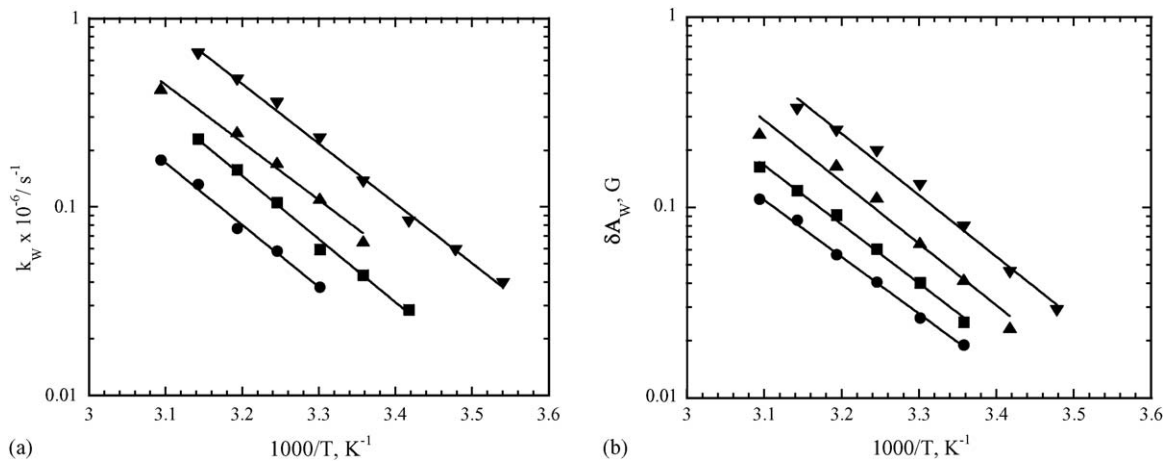

Fig. 6. (a) The rate of transfer of DTBN from water to micelle k_W as a function of 1000/T. (b) The hyperfine coupling constant shift of the water EPR line δA_W as a function of 1000/T. The different lysophospholipid concentrations in micellar solutions are identified as follows: (●) 50 mM, (■) 75 mM, (▲) 100 mM, and (▼) 150 mM. The lines are fits to the Arrhenius equation.

Table 1
Activation energies E_A of pure LMPC and mixed LMPC-SDS micelles

LMPC-SDS/concentration (mM)	E_A from δA_W (kJ/mol)	E_A from δB_W (kJ/mol)
50–0	57.1	62.9
75–0	59.3	61.3
100–0	62.0	58.5
150–0	61.9	60.7
75–25	48.6	48.0
50–50	42.2	37.7

field EPR lines in LMPC micelles decreases with temperature. But in our case this separation cannot be used to find the correct rate of transfer. Again, the reason is that there is no way to measure the effect of the molecular tumbling motion on the position of the micelle high field EPR line. Nevertheless, it is interesting to examine the temperature dependence of the separation as shown in Fig. 6b where we present the hyperfine coupling constant shift of the water EPR line δA_W, which is defined as the difference of the water hyperfine coupling constant A_W measured in the micelle sample and the corresponding hyperfine coupling constant measured in Hepes at the same temperature, as a function of the reciprocal of temperature in Fig. 6b. The solid lines are fits to Eq. (8) giving the values of the activation energies in Table 1. The fits are rather good and as Table 1 shows, the activation energies are similar to those derived from line broadening. This means that the activated process of the combined effects of the shifts of the micelle line and the shift of the water line due to transfer are similar to one another, not really a surprising result.

From Table 1 we can draw two important conclusions regarding the surface properties of pure LMPC and mixed LMPC-SDS micelles. First, although the rate of transfer increases with increasing LMPC concentration, Fig. 4a, the activation energy does not depend on the concentration of LMPC suggesting that the surface of the LMPC micelles does not change with LMPC concentration. This suggests that the size of micelles remains the same. Second, addition of negatively charged SDS molecules to the LMPC micelles reduces the activation energy. This result could mean that the incorporation of negatively charged SDS molecules in the micelle increases the surface area per surfactant molecule of the micelle surface, which would be expected to lower the barrier to the transfer of DTBN. We used the term "compactness" to describe the surface area per surfactant molecule; the smaller the area, the more compact the micelle surface. A decrease in compactness would accompany a decrease in the aggregation number of the mixed micelle; thus, we turned to TRFQ to measure the aggregation numbers of the mixed SDS-phospholipid micelles. Fig. 7 shows the aggregation number of 100 mM pure LMPC, pure SDS and mixed LMPC-SDS micelles at 25 and 35 °C as a function of the concentration of the SDS fraction. The size of mixed micelles linearly decreases from the larger aggregation number of pure LMPC micelles to the smaller aggregation number of pure SDS micelles. This linear decrease in size with increasing fraction of SDS together with the polar nature of SDS indicate that SDS and LMPC molecules in the mixed micelles very likely undergo ideal mixing, without any phase separation. In other words, the average surface area per surfactant molecule increases with increasing fraction of SDS in the mixed LMPC-SDS micelles, while at the same time the size of micelle decreases. We have also found that the aggregation number remains constant at $N = 123 \pm 1$ with LMPC concentration from 10 to 100 mM. The aggregation numbers of pure LMPC micelles at 25 °C measured by TRFQ were 122, 122 and 123 molecules for 10, 50 and 100 mM micellar solutions, respectively. According to a simple model that has been successful in predicting the hydration of globular micelles, the amount of water in the polar shell of the micelle is expected to increase with increasing fraction of SDS (Bales et al., 1998a), and would remain constant with LMPC concentration.

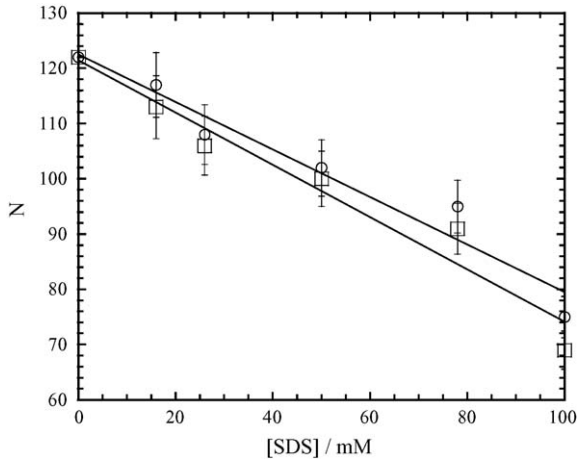

Fig. 7. Aggregation numbers of 100 mM mixed lysophospholipid-SDS micelles as a function of the concentration of the SDS fraction conducted at 25 °C (◯) and 35 °C (□). Error bars are 5% of the values (Ranganathan et al., 1998), and the solid lines are linear least-squares fits to the data.

These predictions of the behavior of the hydration of the micelles may be tested from an analysis of the micelle hyperfine-coupling constant of DTBN, A_M. These results are shown in Fig. 8. Firstly, A_M does not change with the concentration of lysophospholipid in

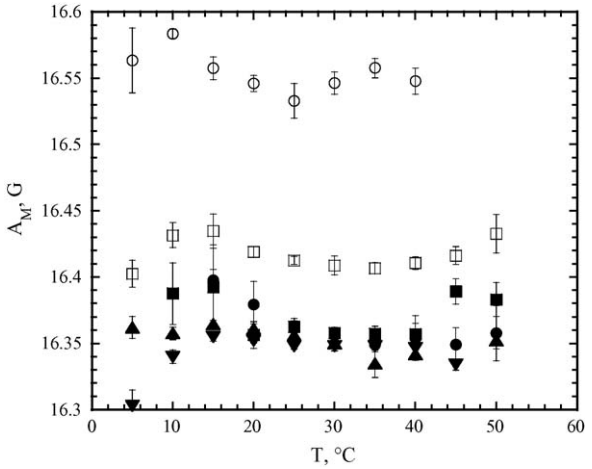

Fig. 8. Hyperfine coupling constant of DTNB originating in the micellar phase, A_M, as a function of temperature. The different lysophospholipid concentrations in pure LMPC micellar solutions are identified as follows: (●) 50 mM, (■) 75 mM, (▲) 100 mM, and (▼) 150 mM. The different lysophospholipid-SDS concentrations in mixed LMPC-SDS micellar solutions are identified as follows: (□) 75 mM LMPC, 25 mM SDS, and (◯) 50 mM LMPC, 50 mM SDS. Error bars are standard deviations of five measurements.

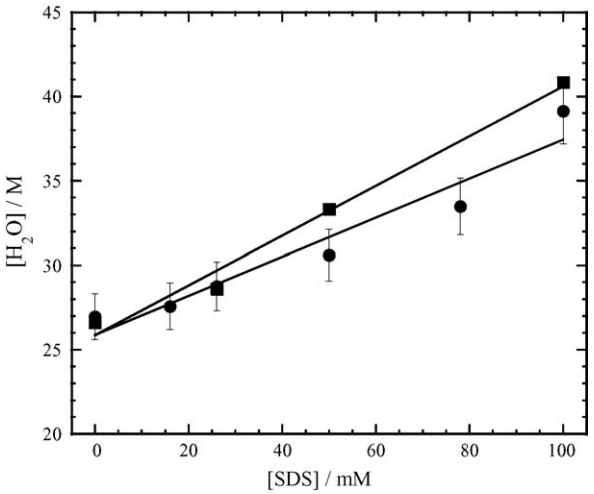

Fig. 9. Effective water concentration in the polar shell of 100 mM mixed lysophospholipid-SDS micelles as a function of the concentration of the SDS fraction at 25 °C. (■) $[H_2O]$ estimated from the hyperfine spacing A_M of DTBN in the micelle; (●) $[H_2O]$ estimated using Eqs. (9)–(12) and the aggregation numbers measured by TRFQ. Error bars are 5% of the values. The solid lines are linear least-squares fits to the data.

the range 50–150 mM in pure LMPC micelles as shown by the solid symbols in Fig. 8. Since the hyperfine coupling constant of a nitroxide spin probe is sensitive to the volume fraction of water encountered by the spin probe (Griffith and Waggoner, 1969) this means that the number of water molecules per unit volume does not change, which in turn implies that the geometry of the polar shell remains the same (Bales et al., 1998a). Therefore, these results strongly indicate that the micelle size does not change as expected for zwitterionic surfactants (Lauterwein et al., 1979). Secondly, the addition of SDS to LMPC micelles increases the value of A_M suggesting an increase in hydration of the polar shell of the micelle. The effective concentration of water in the polar shell of the micelle can be calculated using Eq. (6) from Reference (Peric et al., 2005). Fig. 9 shows the effective concentration of water in the polar shell of mixed LMPC-SDS micelles as a function of the concentration of the SDS fraction at 25 °C. Here, we present only the effective water concentration at 25 °C, since at this temperature the transfer rate is still low and does not appreciably effect the resonant position of the lines. The hydration of the polar shell increases with SDS fraction.

According to a simple geometric hydration model proposed in Bales et al. (1998a), the spherical micelle consists of a shell of headgroups, water and counterions surrounding a core composed of the hydrocarbon tails of the surfactant molecules, which is completely devoid of water. The core in a mixed LMPC-SDS micelle consists of N_{SDS} hydrocarbon tails of SDS and N_{LMPC} hydrocarbon tails of LMPC, where $N_{SDS} + N_{LMPC} = N$, the aggregation number of the mixed LMPC-SDS micelle. Molecular dynamics simulation shows that there is an overlapping region of the core and shell, due to the bending and radial motion of the hydrocarbon tails (MacKerell, 1995). This implies that the core region is reduced by a fraction of the hydrocarbon tail that penetrates the shell. It has been shown that about two methylene groups or one methyl group resides in the polar shell of SDS/heptane micelles (Ranganathan et al., 2001). Thus, assuming that f methylene groups reside in the polar shell, the volume of the core is given by:

$$V_C = (N_{SDS} V_{SDS\text{-}t} + N_{LMPC} V_{LMPC\text{-}t}) - fNV_{CH_2} = \frac{4\pi}{3} r_C^3 \quad (9)$$

where r_C is the radius of the core, $V_{SDS\text{-}t} = 361.8\ Å^3$ is the volume of the hydrocarbon tail of SDS and $V_{LMPC\text{-}t} = 418\ Å^3$ is the volume of the hydrocarbon tail of LMPC. These volumes are calculated using the volume for a CH_2 group of 28.1 $Å^3$ and the volume for a CH_3 group of 52.7 $Å^3$ from Nagle and Tristram-Nagle (2000). Assuming that the thickness of the shell is s, the volume of the micelle becomes:

$$V_M = \frac{4\pi}{3}(r_C + s)^3 = V_C + V_S \quad (10)$$

where V_S is the volume of the shell. The thickness of the polar shell for pure SDS micelles is 5 Å (Bales et al., 1998a), while $s = 9$ Å for pure LMPC micelles (Nagle and Tristram-Nagle, 2000). We make the simplifying assumption that the thickness of the polar shell of mixed micelle changes linearly with the composition of the micelle from 5 to 9 Å (Bales et al., 2001). The volume of the polar shell occupied by the surfactants heads and the hydrocarbon fraction is:

$$V_H = (N_{SDS} V_{SDS\text{-}H} + N_{LMPC} V_{LMPC\text{-}H}) + fNV_{CH_2} \quad (11)$$

where $V_{SDS\text{-}H} = 66.4$ Å^3 is the volume occupied by the sodium sulfate headgroup, and $V_{LMPC\text{-}H} = 319$ Å^3 is the volume occupied by the LMPC head (Nagle and Tristram-Nagle, 2000). The effective concentration of water in the polar shell can then be found by combining Eq. (9) through (11), that is:

$$[H_2O] = \frac{V_S - V_H}{V_S} 55.4[M] \quad (12)$$

The effective concentration of water in the polar shell of mixed LMPC-SDS micelles calculated from the aggregation numbers measured by TRFQ at 25 °C is shown in Fig. 9 as full circles. The only adjustable parameter in the calculation was the number of methylene groups residing in the polar shell, f, which was found to be 1.55. Considering the simplicity of the model, the agreement between the effective water concentration calculated from the hyperfine spacing of DTBN and the effective water concentration obtained from the simple hydration model (Bales et al., 1998a) employing experimental aggregation numbers is excellent.

The presented EPR and TRFQ experimental data, which are consistent with one another, provide strong evidence that the activation energy of DTBN transfer in pure LMPC micelles remains constant with LMPC concentration, because the micelle size and the amount of water in the polar shell of the micelle do not change. In other words, the compactness of the micelle surface remains the same. In mixed LMPC-SDS micelles, the activation energy decreases with the increasing fraction of SDS; that is, as we add more SDS to the LMPC micelles, the compactness of the micelle surface decreases enabling easier DTBN transfer between the polar shell of the micelle and the aqueous phase. This result is reasonable: SDS is anionic while LMPC is zwitterionic, so when SDS molecules are incorporated in the zwitterionic micelle they would tend to move farther apart from each other due to repulsive electrostatic interactions making the surface less compact.

4. Conclusions

Employing improved spectral fitting techniques, we have shown that SPPEPR may be applied with high precision to LMPC and LMPC/SDS mixed micelles. The effective water concentration and the transfer of a solute between lysophospholipid surfactant mixed micelles and the surrounding aqueous phase can be studied with high precision. A model of the mixed LMPC/SDS micelle in which the compactness decreases with SDS molar fraction rationalizes the decrease in activation energy and the increase of transfer rate of the solubilization of DTBN in micelles. This variation in compactness is confirmed by TRFQ. The transfer rate may be measured directly from the broadening of the high field water line, while the activation energy can be measured from both the transfer broadening and the shift of the high field water EPR line. The two measurements are in reasonable agreement with one another. The physicochemical properties of the micelle such as size, hydration and surface compactness of zwitterionic LMPC micelles can be controlled by addition of the anionic surfactant SDS.

Acknowledgments

The authors gratefully acknowledge support from NIH Grants 5 S06 GM48680-09 (BLB) and 3 S06 GM48680-10S1 (MA and MP).

References

Atherton, N.M., Startch, S.J., 1971. E.S.R. Study of aqueous sodium dodecyl sulphate solutions using di-*t*-butyl nitroxide as a probe. JCS Faraday II 68, 374–381.

Bales, B.L., 1989. Inhomogeneously broadened spin-label spectra. In: Berliner, J.L., Reuben, J. (Eds.), Spin Labeling Theory and Applications. Plenum, New York, pp. 77–130.

Bales, B.L., Blum, R.A., Mareno, D., 1992. Solvent and temperature dependence of the hyperfine coupling constants of CTPO. J. Magn. Reson. 98, 299–307.

Bales, B.L., Messina, L., Vidal, A., Peric, M., Nascimento, O.R., 1998a. Precision relative aggregation number determinations of SDS micelles using a spin probe. A model of micelle surface hydration. J. Phys. Chem. B 102, 10347–10358.

Bales, B.L., Peric, M., 1997. EPR line shifts and line shape changes due to spin exchange of nitroxide free radicals in liquids. J. Phys. Chem. B 101, 8707–8716.

Bales, B.L., Peric, M., Lamy-Freund, M.T., 1998b. Contributions to the gaussian line broadening of the proxyl spin probe EPR spectrum due to magnetic-field modulation and unresolved proton hyperfine structure. J. Magn. Reson. 132, 279–286.

Bales, B.L., Ranganathan, R.L., Griffiths, P.C., 2001. Characterization of mixed micelles of SDS and a sugar-based nonionic surfactant as a variable reaction medium. J. Phys. Chem. B 105, 7465–7473.

Bales, B.L., Shahin, A., Lindblad, C., Almgren, M., 2000. Time-resolved florescence quenching and electron paramagnetic reso-

nance studies of the hydration of lithium dodecyl sulfate micelles. J. Phys. Chem. 104, 256–263.
Bergstrand, N., Edwards, K., 2001. Aggregate structure in dilute aqueous dispersions of phospholipids, fatty acids, and lysophospholipids. Langmuir 17, 3245–3253.
Berliner, L.J. (Ed.), 1976. Spin Labeling: Theory and Applications. Academic Press, New York.
Beswick, V., Guerois, R., Cordier-Ochsenbeim, E., Cole, Y.M., Tam, H.D., Tostain, J., Noel, J.P.S.A., Neumann, J.M., 1999. Dodecylphosphocholine micelles as a membrane-like environment: new results from NMR relaxation and paramagnetic relaxation enhancement analysis. Eur. Biophys. J. 28, 48–58.
Bryson, E.A., Rankin, S.E., Carey, M., Watts, A., Pinheiro, T.J.T., 1999. Folding of apocytochrome *c* in lipid micelles: Formation of á-helix precedes membrane insertion. Biochemistry 38, 9758–9767.
Cevc, G. (Ed.), 1993. Phospholipids Handbook. Marcel Dekker, New York.
Deems, R.A., 2000. Interfacial enzyme kinetics at the phospholipid/water interface: practical considerations. Anal. Biochem. 287, 1–16.
Garavito, R.M., Ferguson-Miller, S., 2001. Detergents as tools in membrane biochemistry. J. Biol. Chem. 276, 32403–32406.
Gennis, R.B., 1989. Biomembranes Molecular Structure and Function. Springer–Verlag, New York.
Gil, T., Ipsen, J.H., Mouritsen, O.G., Sabra, M.C., Sperotto, M.M., Zuckermann, M.J., 1998. Theoretical analysis of protein organization in lipid membranes. Biochim. Biophys. Acta 1376, 245–266.
Goñi, F.M., Alonso, A., 2000. Spectroscopic techniques in the study of membrane solubilization, reconstitution and permeabilization by detergents. Biochim. Biophys. Acta 1508, 51–68.
Gow, A., Auton, W., Smith, R., 1990. Interactions between bovine myelin basic protein and zwitterionic lysophospholipids. Biochemistry 29, 1124–1147.
Gow, A., Winzor, D.J., Smith, R., 1987. Equilibrium binding of myristoyllysophosphatidylcholine to bovine myelin basic protein: an example of ligand-mediated acceptor association. Biochemistry 26, 982–987.
Griffith, O.H., Dehlinger, P.J., Van, S.P., 1974. Shape of the hydrophobic barrier of phospholipid bilayers (evidence for water penetration in biological membranes). J. Membr. Biol. 15, 159–192.
Griffith, O.H., Waggoner, A.S., 1969. Nitroxide free radicals: spin labels for probing biomolecular structure. Acc. Chem. Res. 2, 17–24.
Gutowsky, H.S., Holm, C.H., 1956. Rate processes and nuclear magnetic resonance spectra. II. Hindered internal rotation of amides. J. Chem. Phys. 25, 1228–1234.
Halpern, H.J., Peric, M., Yu, C., Bales, B.L., 1993. Rapid quantitation of parameters from inhomogeneously broadened EPR spectra. J. Magn. Reson. A103, 13–22.
Hayashi, H., Yamanaka, T., Miyajima, M., Imae, T., 1994. Aggregation numbers and shapes of lysophospatidylcholine and lysophospatidylethanolamine micelles. Chem. Lett. 23, 2407–2410.
Hubbell, W.L., McConnell, H.M., 1968. Spin-label studies of the excitable membranes of nerve and muscle. Proc. Natl. Acad. Sci. U.S.A. 61, 12–26.
Hyde, J.S., Subczinski, W.K. (Eds.), 1989. Spin-Label Oximetry. Plenum, New York.
Infelta, P.P., Grätzel, M., Thomas, J.K., 1974. Luminescence decay of hydrophobic molecules solubilized in aqueous micellar systems. A kinetic model. J. Phys. Chem. 78, 190–195.
Lauterwein, J., Bosch, C., Brown, L., 1979. Physicochemical studies of the protein–lipid interactions in melittin-containing micelles. Biochim. Biophys. Acta 556, 244–264.
le Maire, M., Champeil, P., Møller, J.V., 2000. Interaction of membrane proteins and lipids with solubilizing detergents. Biochim. Biophys. Acta 1508, 86–111.
MacKerell, A.D.J., 1995. Molecular dynamics simulation analysis of a sodium dodecyl sulfate micelle in aqueous solution: decreased fluidity of the micelle hydrocarbon interior. J. Phys. Chem. 99, 1845–1855.
McConnell, H.M., 1958. Reaction rates by nuclear magnetic resonance. J. Chem. Phys. 28, 430–431.
Nagle, J.F., Tristram-Nagle, S., 2000. Structure of lipid bilayers. Biochim. Biophys. Acta 1469, 159–195.
Nordio, P.L., 1976. General magnetic resonance theory. In: Berliner, J.L. (Ed.), Spin Labeling Theory and Applications. Academic Press, New York, pp. 5–52.
Oakes, J., 1972. Magnetic resonance studies in aqueous systems. JCS Faraday II 68, 1464–1471.
Peric, M., Alves, M., Bales, B.L., 2005. Precision parameters from spin-probe studies of membranes using a partitioning technique. Application to two model membrane vesicles. Biochim. Biophys. Acta 1669, 116–124.
Peric, M., Bales, B.L., 2004. Lineshapes of spin exchange broadened EPR spectra. J. Magn. Reson. 169, 27–29.
Plachy, W.Z., Windrem, D.A., 1977. A Gas-permeable ESR sample tube. J. Magn. Reson. 27, 237–239.
Ranganathan, R., Peric, M., Bales, B.L., 1998. Time-resolved fluorescence quenching measurements of the aggregation numbers of normal sodium alkyl sulphate micelles well above the critical micelle concentrations. J. Phys. Chem. B 102, 8436–8439.
Ranganathan, R., Peric, M., Medina, R., Garcia, U., Bales, B.L., Almgren, M., 2001. Size, hydration, and shape of SDS/heptane micelles investigated by time-resolved fluorescence quenching and electron spin resonance. Langmuir 17, 6765–6770.
Rankin, S.E., Watts, A., Pinheiro, T.J.T., 1998. Electrostatic and hydrophobic contributions to the folding mechanism of apocytochrome *c* driven by the interaction with lipid. Biochemistry 37, 12588–12595.
Riske, K.A., Nascimento, O.R., Peric, M., Bales, B.L., Lamy-Freund, M.T., 1999. Probing DMPG vesicle surface with a cationic aqueous soluble spin label. Biochim. Biophys. Acta 1418, 133–146.
Rogers, M.T., Woodbrey, J.C., 1962. A proton magnetic resonance study of hindered internal rotation in some substituted *N*,*N*-dimethylamides. J. Phys. Chem. 66, 540–546.
Schreier, S., Polnaszek, C.F., Smith, I.C.P., 1978. Spin labels in membranes problems in practice. Biochim. Biophys. Acta 515, 375–436.
Shimshick, E.J., McConnell, H.M., 1973. Lateral phase separations in phospholipid membrane. Biochemistry 12, 2351–2360.
Smirnova, T.I., Smirnov, A.I., Clarkson, R.B., Belford, R.L., 1995. W-band (95 GHz) EPR spectroscopy of nitroxide radicals with complex proton hyperfine structure: fast motion. J. Phys. Chem. 99, 9008–9016.
Stafford, R.E., Dennis, E.A., 1988. Lysophospholipids as biosurfactants. Colloids Surf. 30, 47–64.
Tachiya, M., 1975. Applications of a generating function to reaction in micelles. Kinetics of quenching of luminescent probes in micelles. Chem. Phys. Lett. 33, 289–292.
Uematsu, S., Uchida, T., Kinoshita, A., Kimura, F., Akahori, Y., 1995. Relation between micellar structure of model bile and activity of esterase. Biochim. Biophys. Acta 1258, 122–134.

Weil, J.A., Bolton, J.R., Wertz, J.E., 1993. Electron Paramagnetic Resonance: Elementary Theory and Practical Applications. John Wiley and Sons Inc., New York.

Weltzien, H.U., Arnold, B., Reuther, R., 1977. Quantitative studies on lysolecithin-mediated hemolysis use of ether-deoxy lysolecithin analogs with varying aliphatic chain lengths. Biochim. Biophys. Acta 466, 411–421.

Windle, J.J., 1981. Hyperfine coupling constants for nitroxide spin probes in water and carbon tetrachloride. J. Magn. Reson. 45, 432–439.